AIAA Atmospheric Flight Mechanics Conference and Exhibit
18 - 21 August 2008, Honolulu, Hawaii

AIAA 2008-6207

Enhancement of the Nonlinear OLOP-PIO-Criterion Regarding Phase-Compensated Rate Limiters

Daniel Ossmann[1]
DLR - German Aerospace Center, Institute of Flight Systems, 85077 Manching, Germany

Matthias Heller[2]
EADS Military Air Systems, 85077 Manching, Germany

Oliver Brieger[3]
DLR - German Aerospace Center, Institute of Flight Systems, 85077 Manching, Germany

The unique dynamic coupling effects between airframe, flight control system, and the pilot of modern, highly or super-augmented aircraft introduce new stability and handling qualities problems which do not occur on conventional airplanes. In particular, phenomena leading to a destabilization of the closed-loop system consisting of the airframe, the control and stability augmentation system, and the pilot, triggered by an undesired and unexpected interaction between pilot and augmented aircraft dynamics are known to be very dangerous for the aircraft and crew. They are commonly referred to as Pilot Involved or Pilot-In-the-Loop Oscillations. This paper focuses on the enhancement of the so called Open-Loop-Onset-Point-criterion, originally developed to predict PIO-susceptibility due to nonlinear effects such as position and non-phase-compensated rate limiting. The criterion is modified to also cover phase-compensated rate limiters, which are now commonly found in modern flight control systems.

Nomenclature

ATTAS	=	Advanced Technologies Testing Aircraft System
CCV	=	Control Configured Vehicle
DLR	=	Deutsches Zentrum für Luft- und Raumfahrt (German Aerospace Center)
EADS	=	European Aeronautic Defence and Space Company
FBW	=	Fly-By-Wire
FCS	=	Flight Control System
PIO	=	Pilot-in-the-Loop Oscillations
PVS	=	Pilot-Vehicle-System
A_0, φ_0	=	Magnitude and phase at the OLOP
A_N	=	Integral (area) of the approximated phase-compensated rate limiter (sinusoidal) output y_N
A_1-A_3	=	Integrals (areas) of the phase-compensated rate limiters output
com	=	Commanded signal
ΔA_h /ΔA_{pk}	=	Amplitude difference of in- and output of a conventional/phase-compensated rate limiter
dem	=	Demanded signal
F	=	Transfer function
F_{es}	=	Stick force
K_P	=	Pilot gain
lim	=	Limited signal
ν	=	Rate limit activation ratio

[1]Research Scientist, Flight Test Group Manching, Ingolstadt/Manching Airbase, Member.
[2]Expert Advisor Flight Dynamics, Flight Dynamics.
[3]Group Leader, Flight Test Group Manching, Ingolstadt/Manching Airbase, Member.

$N(j\omega, \hat{u})$ = Overall rate limiter describing function
$N_I(j\omega, \hat{u})$ = Describing function of an inactive (phase-compensated) rate limiter
$N_{II}(j\omega, \hat{u})$ = Describing function of an activated (phase-compensated) rate limiter
OLOP = Open-loop Onset Point
ω = Frequency
ω_c = Crossover frequency
ω_{onset} = Onset-frequency
φ_c = Crossover phase angle
$\Delta\varphi_h$ = Phase loss of a conventional rate limiter
R = Rate limit
S_{NII} = Slope of the (phase-compensated) describing function in the Nichols chart
sen = Sensor signal
T = Signal period
t_a, t_b = Activation/deactivation times
Θ = Pitch angle
η = Elevator deflection angle
$u_{\max}$ = Input amplitude
u_{RLin} = Rate limiter input
y_h, y_{pk} = Output of a conventional/phase-compensated rate limiter
y_N = Approximated (sinusoidal) output signal of a phase-compensated rate limiter

I. Introduction

THE continuous evolution of modern 'Fly-by-Wire' (FBW) Flight Control Systems (FCS) in the last decades has enabled the optimization of the conceptual design with respect to aircraft performance without having to make concessions regarding stability and flying qualities. These highly control configured vehicles (CCV) have to pass an extensive analysis process to guarantee stability and robustness of the closed-loop (aircraft + controller + pilot) system over the entire flight envelope. This process requires a complete evaluation of the system in numerous operating conditions. Inadvertent pilot vehicle coupling effects so called 'Pilot Involved Oscillations' (PIO),[11] leading to a destabilization of the pilot-aircraft-system are still a subject-matter within the control systems engineering and handling qualities communities due to its criticality and complexity. PIOs are divided into four categories, allowing a clearer differentiation:

Category I is based on essentially linear pilot and aircraft dynamics, with PIO development being associated with high open-loop system gain and excessive phase lags in the effective vehicle dynamics.

Category II assumes a quasi-linear system behavior, but considers position and rate limiting as dedicated nonlinearities and potential cause for PIOs. Such phenomena are usually extremely dangerous, since they involve large amplitudes so that rate and position limiting become effective and may cause an abrupt reduction of closed-loop system bandwidth, which can lead to catastrophic accidents (e.g. PIO accident of the JAS–39 Gripen).

Position and rate limiters are naturally defined by the physical constraints of actuation systems due to their geometry and their mechanical characteristics. Artificial rate and position limiters are implemented into the FCS to protect actuation systems from physical damage. Their defined limits are in general lower than the physical ones, which has different reasons. An artificial position limiter prevents the piston from hitting the mechanical stop at full speed, which can lead to tremendous mechanical damage and reduces the durability of the actuator dramatically. Software-imposed rate limits are implemented in modern control systems to protect the hydraulic system from excessive pressure losses and thereby induced overload phenomena. The general drawback, however, is that they represent nonlinear elements which can influence the system stability, once they are activated.

Category III PIOs address any kind of nonlinear system behavior, which can be induced by the aircraft but also by the pilot. Examples are mode switching events within the control laws, abrupt changes in the aerodynamic properties, for instance due to reconfiguration or the release of external stores, or transitions in pilot behavior.

Category IV has been introduced recently and accounts for coupling effects between pilot inputs and the aircraft structural modes.

The introduction of FBW flight control systems initially resulted in repeated occurrences of Cat. I PIOs. The associated deficiencies, i.e. insufficient gain margins and excessive phase lags have mostly been understood and solved throughout the ongoing progress in the development of full authority flight control systems in the last decades. Analysis of time histories of recently observed PIO events and accidents have identified rate limiting as the primary cause for the system destabilisation, which yielded the necessity for a new criterion, taking these nonlinear

effects into account. The Open-Loop-Onset-Point (OLOP) criterion has been developed using the describing function technique and the application of frequency domain methods.[1]

Generally, it has to be noted that an activated rate limiter is not always the trigger for a PIO incident, but can also be the result of a fully developed PIO, destabilizing the system even further. Nevertheless, some spectacular PIO events (e.g. JAS–39 Gripen) can be ascribed to the activation of the rate limiter and the subsequent saturation as primary triggering event. Therefore, it is essential to use the OLOP-criterion in the early stages of the design phase of the FCS in order to identify and suppress these nonlinear effects.

A result of these analysis methods and the lessons learned from documented CAT II PIO events has been the introduction of so called phase-compensated rate limiters,[12,13] which minimize the added phase lag – the primary cause for Cat II PIOs – but reduce the output amplitude. Therefore, this paper focuses on the system-theoretical background and the effects of a phase-compensated rate limiter on the closed-loop system. Potentially remaining stability problems are discussed and finally an enhancement of the OLOP-criterion is proposed to enable the application of this powerful handling-qualities criterion to systems featuring phase-compensated rate limiters. To validate the proposed modifications, the new criterion is applied to three aircraft models featuring highly sophisticated control law structures with phase-compensated rate limiters. The predictions using the enhanced criterion are then compared against the results of nonlinear simulations.

II. The 'Classical' OLOP-Criterion

A. Theoretical Background

Although Cat. II PIOs describe oscillations due to the nonlinear effects of rate and/or position limiting, the OLOP-criterion is based on linear analysis and the associated frequency response of the aircraft. However, it has to be noted that linear effects are not considered and therefore no correlations to Cat. I PIO prediction criteria (e.g. Neal-Smith Criterion, Bandwidth Criterion, Gibson's Phase Rate Criterion, etc.) exist.[2]

(Quasi-) linear system theory can be applied, as the OLOP-criterion makes extensive use of the describing function technique. Describing functions constitute a useful method to approximate a nonlinear element by an amplitude-dependent frequency response. For fully activated rate limiters the describing function $N(j\omega)$ depends on the frequency ω and the input amplitude u_{RLin}, where the amplitude-dependency is included in the definition of the so called onset-frequency ω_{onset}, denoting the frequency at which the rate limiter becomes active for the first time:[1,3,6]

$$N(j\omega) = \frac{4\omega_{onset}}{\pi\omega} e^{-j\arccos\left(\frac{\pi\omega_{onset}}{2\omega}\right)} \tag{2.1}$$

with

$$\omega_{onset} = R / u_{RLin} \tag{2.2}$$

In Eq. (2.2) R denotes the rate limit value. Investigations by the German Aerospace Center (DLR) have identified so called open-loop gradients in the frequency response as soon as the limiter is activated and the system may be driven unstable. It has been proven that these gradients, which mainly introduce a significant, additional phase lag into the system correlate with the location of the OLOP in the Nichols chart.[1] The phase loss in the open-loop response may lead to an increase of the closed-loop amplitude, which can amplify the input amplitude and thus introduce additional phase lag into the system. This in turn may trigger or exacerbate an existent saturation condition possibly leading to closed-loop instability. Whether this additional phase lag causes an increase of the closed-loop amplitude or not depends on the location of the OLOP in the Nichols chart (Fig. 1). If the OLOP is located above the boundary (proposed by H. Duda in Ref. 1 to discriminate between PIO-prone and PIO-resistant configurations) a change in the open-loop phase causes a significant increase in closed-loop amplitude due to the nature of the *M*-circles (lines of constant closed-loop amplitude) as illustrated in Fig. 1. For an OLOP located clearly below the boundary the increasing open-loop phase delay does not cause a considerable increase in closed-loop gain, and hence has no destabilizing effect on the aircraft-pilot-system.

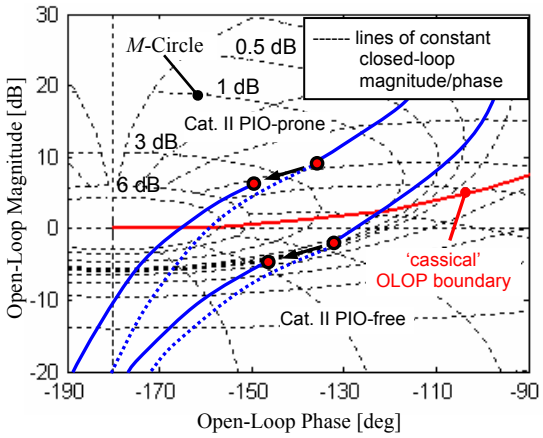

Figure 1. Physical interpretation of the OLOP-parameter.

B. Evaluation Procedure

For the application of the OLOP-criterion, the use of the describing function technique is not required. A linear model of the aircraft including the flight control system, the location of the relevant rate limiter, and information about maximum stick deflections and maximum rates must be available. The procedure for the evaluation of the 'classical' OLOP-criterion is summarised below:

Step 1: First a simple pilot gain model is calculated. This pure gain model can be used because it is assumed that the pilot, after a period of adjustment, exhibits synchronous precognitive behavior, when encountering a fully developed PIO, duplicating the sinusoidal character of the aircraft response. The transfer function from the stick input (deflection or force) to the pitch attitude Θ is used to determine the pilot gain:

$$K_P(\varphi_c) = \left| F_{stick}^{\Theta}(\omega_c) \right| = 1 \tag{2.3}$$

Here ω_c is the crossover frequency where the attitude-to-stick transfer function has a specific phase angle φ_c. Resulting pilot gains for varying crossover phase angles φ_c between -90 deg to -130 deg for the pitch axis and -110 deg to -160 deg for the roll axis should be investigated to cover a wide range of possible pilot gains.

Step 2: Calculation of the frequency response from the stick force (or deflection) F_{es} to the input of the rate limiter (here: unlimited elevator deflection command δ_e) for the linear closed-loop system:

$$F_{stick}^{\delta_e}(j\omega) = \delta_e / F_{es} \tag{2.4}$$

Step 3: Determination of the onset-frequency ω_{onset} by using the frequency response from the stick input to the rate limiter input of the closed-loop system (without pilot):

$$\underbrace{u_{\max} \cdot \left| F_{stick}^{RLin}(j\omega) \right|}_{u_{RLin}} = R / \omega_{onset} \tag{2.5}$$

Step 4: Finally, the linear OLOP transfer function is derived, being the open-loop transfer function from the rate limiter output to the rate limiter input, meaning that the closed-loop system is cut directly at the rate limiting element. For the calculation of the OLOP transfer function, the limiter has to be removed, and only the frequency at which the limiter is initially activated is taken into account for the evaluation of the criterion. The OLOP-parameter is defined as phase $\varphi_0(\omega)$ and magnitude $A_0(\omega)$ of the OLOP transfer function at the onset-frequency ω_{onset}:

$$\text{OLOP} = [\varphi(\omega_{onset}), A_0(\omega_{onset})] \tag{2.6}$$

This procedure is applicable to the two typical rate limiter locations (stick-command shaping in the feedforward path and actuator limitation in the feedback loop, see Fig. 2) and to both the pitch and the roll axis. The following research focuses on the analysis of potential system destabilizations due to saturations in the inner control loop of the pitch axis.

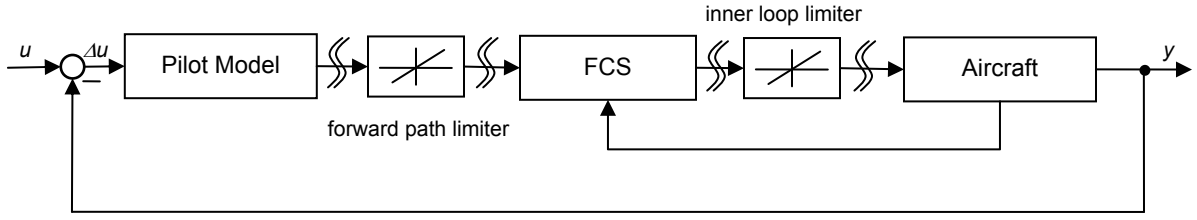

Figure 2. Possible rate limiter positions within the PVS.

For validation purposes a nonlinear simulation is conducted, in which the rate limiters are taken into account. A generic excitation function is defined in such a way, that from initial steady state sinusoidal dynamics in interval I the rate limiter is activated during the second interval where the frequency exceeds ω_{onset} by a factor of 1.1, as depicted in Fig. 3.[1,6] If the aircraft response converges to its steady state condition and the induced oscillation ceases after the exciting function is terminated, the overall system can be considered as PIO-free with a high level of confidence. For phase-compensated rate limiters basically the same excitation function is used, however, interval II is prolonged to cover five periods instead of only two because the open-loop gradient related to phase-compensated rate limiters is characterized by a distinctive magnitude reduction. For systems with an OLOP location 'far right' from the critical point (0 dB / -180 deg) in the Nichols chart the reduction in open-loop magnitude may lead to a less pronounced destabilization due to the temporary closed-loop increase in system amplitude or may even have no effect at all (see Nichols-*M*-circles, Fig. 4) compared to conventional non-compensated rate limiters. Therefore, a prolonged excitation enables greater insight into the developing system dynamics.

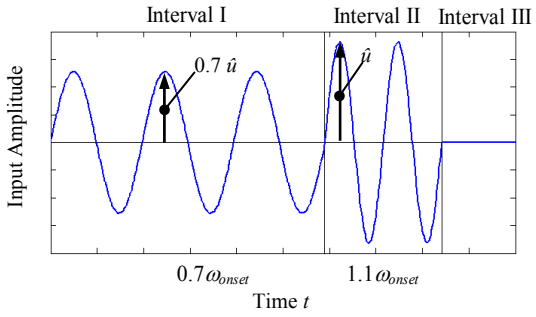

Figure 3. PVS input signal for the nonlinear simulation.

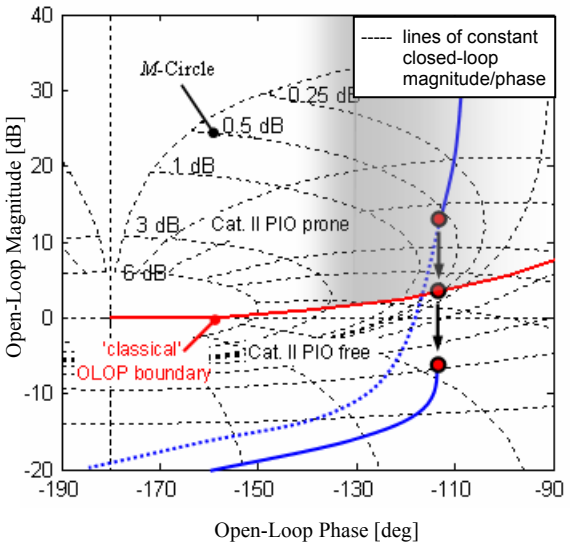

Figure 4. Assumed area of reduced Cat. II PIO susceptibility.

III. Phase-Compensated Rate Limiters

After numerous Cat. II PIO incidents and accidents in the 90s, the need for control law modifications to suppress Cat. II PIO tendencies became evident. This led to the development of the OLOP-criterion, presented in the last paragraph. For already operational aircraft this criterion came too late. To avoid a complete control law redesign, other solutions had to be found. Since the extensive phase lag was identified as the main cause for Cat. II PIOs, the idea arose to compensate this phase lag or to modify the rate limiter in such a way that no additional phase lag is introduced into the system.[13] This can be achieved by implementing phase-compensated rate limiters into the FCS, where the input and output of the rate limiter exhibits identical algebraic signs opposed to non-compensated rate limiters as depicted Fig. 5.

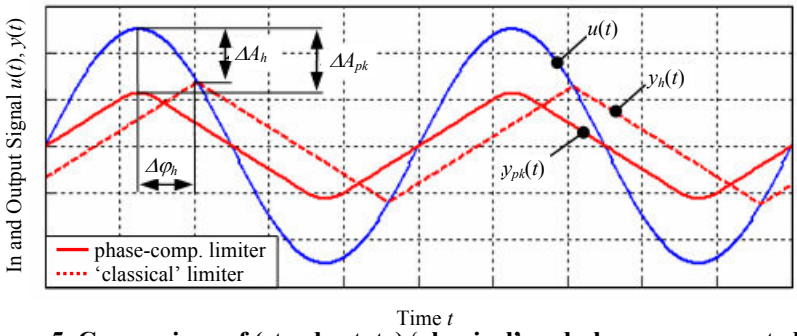

Figure 5. Comparison of (steady state) 'classical' and phase-compensated rate saturation for sinusoidal input signal.

A. Characteristics

For a 'classical', non phase-compensated rate limiter three different modes of activation can be distinguished for a sinusoidal input.[1] For input frequencies below ω_{onset} the rate limiter's output follows the input signal at any time, the limiter is not activated. For frequencies above $1.86\omega_{onset}$, as described in Ref. 1, the rate limiter is fully activated and only discrete intersections between the input $u(t)$ and output signal $y_h(t)$ are present, exhibiting the typical sawtooth characteristic. Between ω_{onset} and $1.86\omega_{onset}$ there is a a hybrid mode, where the output of the limiter can follow the input only partially. In contrast, a phase-compensated rate limiter only operates in two different modes. Either the limiter is not activated and its output $y_{pk}(t)$ is equal to the input, or it is saturated and therefore only discrete intersections every half period exist. In Fig. 5 the output signals of a fully activated phase-compensated and of a conventional rate limiter are shown. Clearly visible is the phase lag $\Delta\varphi_h$ of the non-compensated limiter, resulting in a high PIO Cat. II susceptibility, whereas the compensated rate limiter shows a more significant amplitude reduction ΔA_{pk}, however, nearly without any phase lag. A more detailed illustration of the time history of a phase-compensated rate limiter is depicted in Fig. 6. From $t = 0$, where the input $u(t)$ has its maximum rate, the rate limiter remains activated until the rate of the input signal $u(t)$ decreases to the rate limit value R at t_a. From this point on up to t_b the output follows the input without any phase lag, but, with a constant difference in amplitude ΔA. At t_b the rate of the input signal reaches the minimum permitted rate $-R$ and the rate limit is activated once again until reaching $T/2 + t_a$. Since the determination of t_a and t_b is essential for the derivation of an adequate describing function for the phase-compensated rate limiter, they are calculated below.

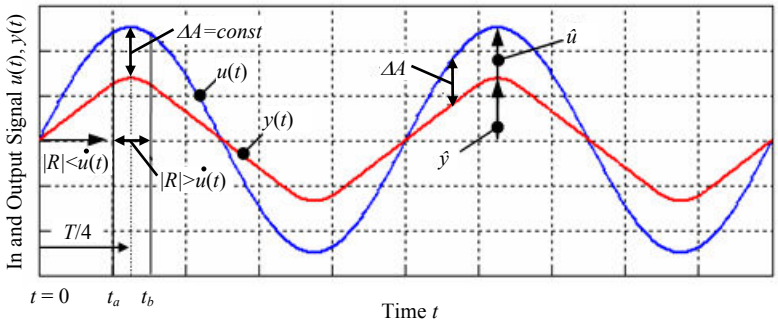

Figure 6. Time history of phase-compensated rate limiting.

At t_a (resp. t_b) the rate of the (sinusoidal) input signal is equal to the maximum rate $\pm R$:

$$\dot{u}(t_{a/b}) = \hat{u}\,\omega\cos(\omega t_{a/b}) = \pm R \tag{3.1}$$

Solving Eq. (3.1) for t_a and t_b and considering their half-periodic property gives:

$$\begin{aligned} t_a &= \frac{1}{\omega}\arccos\left(\frac{R}{\omega\,\hat{u}}\right) + n\,\frac{T}{2} \quad n = 0,1,2,... \\ t_b &= \frac{1}{\omega}\arccos\left(\frac{-R}{\omega\,\hat{u}}\right) + n\,\frac{T}{2} \quad n = 0,1,2,... \end{aligned} \tag{3.2}$$

Eq. (3.2) is valid for frequencies $\omega \geq \omega_{onset}$. The output of the rate limiter, and consequently the calculated activation and deactivation times t_a and t_b, depend on the defined rate limit $\pm R$, the input amplitude $\hat{u}$ and the frequency ω. With the given (constant) input amplitude and a defined rate limit, the output signal of the rate limiter can be approximated by a sawtooth function for high frequencies ($\omega >> \omega_{onset}$). The degree ν to which the rate limiter is activated, equivalent to the extent to which the initial sinusoidal input has transformed into the sawtooth function, can be determined, considering the symmetry of the output signal around $T/4$, by the following expression:

$$\nu = t_a / (T/4) = 2\, t_a\, \omega / \pi \tag{3.3}$$

The frequency-dependent plot in Fig. 7 shows that t_a initially is increasing, starting from the onset-frequency ω_{onset}, as the maximum rate $\dot{u}_{\max}$ of the input signal u increases. However, at higher frequencies, it can be observed, with the period T (resp. $T/4$) further decreasing, that the (absolute) activation time t_a reduces once again. As the frequency of the input signal increases the activation ratio ν converges to a value of 1 and the output signal can therefore be approximated as a sawtooth function. Correspondingly, the same trend regarding ν can be observed when varying the maximum rate R as described in Eq. (3.2) and Eq. (3.3).

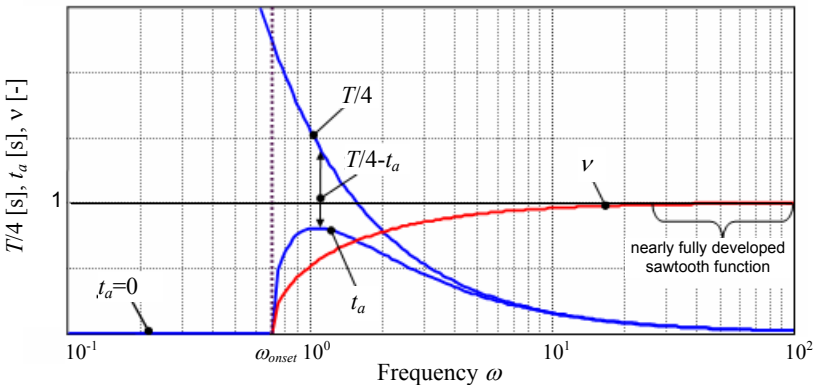

Figure 7. Dependency of the activation ratio ν on ω.

B. Derivation of an Appropriate Describing Function

In order to be able to analyse the phase-compensated rate limiter with common tools like the Nichols chart, a describing function needs to be derived. By means of this approximated transfer function it is then possible to identify the explicit direction of the open-loop gradient, which is the basis for the adaptation of the OLOP-criterion. The determination of a suitable describing function for the activated, phase-compensated rate limiter is achieved by approximating the output signal of the rate limiter by a sinusoidal function having the identical signal energy content. As signals with the same energy enclose identical areas around the time axis, the corresponding integrals of the signals are compared to each other. In Fig. 8 the input signal $u(t)$, the rate limiter output signal $y_{pk}(t)$ and the approximated sinusoidal signal $y_N(t)$ for a given frequency ω are depicted. The already discussed symmetry of the signal around $T/4$ allows a simplified approach and therefore only the first quarter of the period is considered.

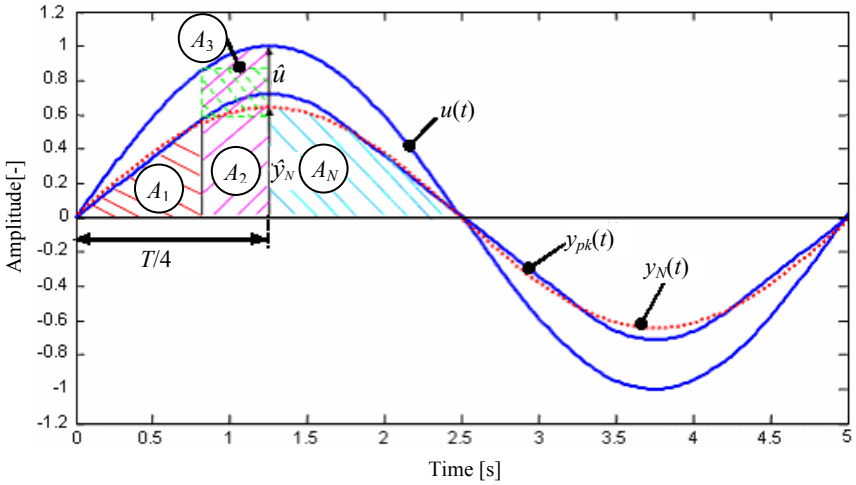

Figure 8. Comparison of the signal energies via the curve areas.

Equating the integral A_N of the sinusoidal signal y_N and the area below the rate limited signal from $t = 0$ to $t = T/4$ leads to:

$$\underbrace{\hat{y}_N \int_0^{T/4} \sin(\omega t)\,dt}_{A_N} = \underbrace{\int_0^{t_a} R\,t\,dt}_{A_1} + \underbrace{\hat{u} \int_{t_a}^{T/4} \sin(\omega t)\,dt}_{A_2} - \underbrace{\left\{\left[\hat{u}\sin(\omega t_a) - R\,t_a\right]\left[\frac{T}{4} - t_a\right]\right\}}_{A_3} \tag{3.4}$$

Solving Eq. (3.4) for the required amplitude $\hat{y}_N$ of the sinusoidal signal gives:

$$\hat{y}_N = \omega\left[R\left(\frac{T\,t_a}{4} - \frac{t_a^2}{2}\right) + \hat{u}\sin(\omega t_a)\left(t_a - \frac{T}{4}\right)\right] + \hat{u}\cos(\omega t_a) \tag{3.5}$$

The required describing function $N_{II}(j\omega, \hat{u})$ for the activated limiter, expressing the ratio of the (approximated) rate limiter output y_N to the input signal u, can now be formulated, considering that no phase lag is present, i.e. $\Delta\varphi = 0$:

$$N_{II}(j\omega,\hat{u}) = \frac{y_N}{u} = \left|N_{II}(j\omega,\hat{u})\right| e^{-j\Delta\varphi} \overset{\Delta\varphi=0}{=} \left|N_{II}(j\omega,\hat{u})\right| = \frac{\hat{y}_N}{\hat{u}} \tag{3.6}$$

The describing function $N_{II}(j\omega, \hat{u})$ for the activated (phase-compensated) rate limiter is now determined. The formulation of the describing function for frequencies lower than ω_{onset} is trivial, since the output signal follows the input at any time, and hence, can be expressed by

$$N_I(j\omega,\hat{u}) = \frac{y_N}{u} = \frac{y}{u} = 1 \tag{3.7}$$

The overall describing function $N(j\omega)$ can be plotted in a Bode diagram as depicted in Fig. 9. For the illustrated plot an onset-frequency of 1 rad/s was chosen. Before reaching the onset-frequency ω_{onset} no reduction in amplitude can be observed, since no saturation occurs. As soon as the limiter is activated, Eq. (3.6) becomes applicable. Over the entire frequency range the phase lag remains zero. The significant amplitude reduction becomes the main driver for further handling and flying qualities analyses and the adaptation of the OLOP-criterion. To what extent the discussed behaviour of the phase-compensated rate limiter, interacting with a controlled system, influences stability and the Cat. II PIO susceptibility is discussed in the next section. Therefore, it is essential to analyze the influence of the position of the OLOP-parameter in the Nichols chart and the associated open-loop gradient on the system behaviour, as it has previously been done for a conventional rate limiter during the development of the 'classical' OLOP-criterion.

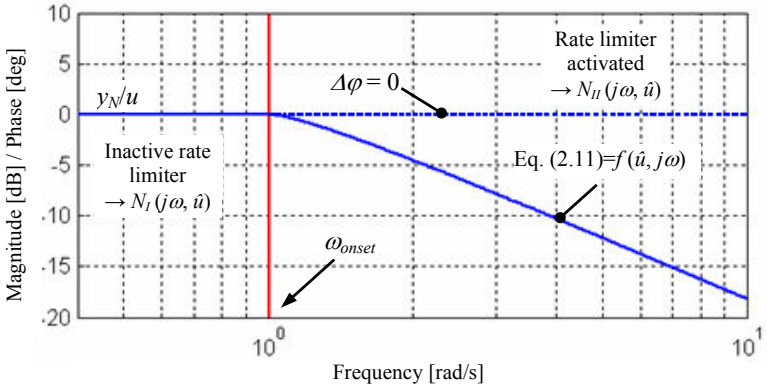

Figure 9. Bode plot of a phase-compensated rate limiter.

IV. Enhancement of the OLOP-Criterion for Phase-Compensated Rate Limiters

A. Proposal of a New Boundary Considering the Direction of the Open-loop Gradient

For an activated conventional rate limiter the saturation provokes an additional open-loop gradient in phase and magnitude. Extensive research in Ref. 1 has proven that the direction of this gradient correlates with the open-loop phase and amplitude changes of the rate limiter's quasi-linear describing function in the Nichols chart. Similarly, the slope of the describing function of the phase-compensated rate limiter also needs to be determined; however, this is straightforward and can be easily obtained with Eq. (2.13), as no phase loss is encountered during activation.[7]

$$S_{NII} = \frac{\Delta\left|N_{II}(j\omega)\right|}{\arg(N_{II}(j\omega))} = -\infty \tag{4.1}$$

With the characteristics of the nonlinear open-loop gradient now being defined, its influence on the system's closed-loop stability can be analyzed. Depending on the OLOP location in the Nichols chart the closed-loop amplitude either increases or decreases. By making use of the *M*-circle theory,[14] describing constant closed-loop amplitude, a boundary can be drawn to discriminate between these two regions. This boundary is defined by the line of constant closed-loop magnitude slope expressed by Eq. (4.1) (line of negative infinite slope of the *M*-circles). It constitutes the first proposal for the modified OLOP-boundary for phase-compensated rate limiters, since activation below this line reduces the closed-loop amplitude and therefore cannot lead to closed-loop instability (see Fig. 10). An OLOP above this boundary on the other hand may increase the closed-loop amplitude, influencing the input of the rate limiter due to the FCS feedback structure. As a result the system saturation may be exacerbated leading to a destabilization.[1] Compared to the OLOP-boundary for conventional rate limiters the proposed boundary shows – as expected – that a phase-compensated rate limiter is less critical with respect to Cat. II PIOs. However, the 'classical' OLOP-boundary is the result of a modified line of constant closed-loop magnitude slope, defined by the initial gradient of the related describing function in the Nichols chart (see Fig. 10 and refer to Ref. 1 and Ref. 10). Since the classical OLOP boundary was validated using simulations and flight test data this procedure is also applied to verify the newly proposed boundary for phase-compensated rate limiters.

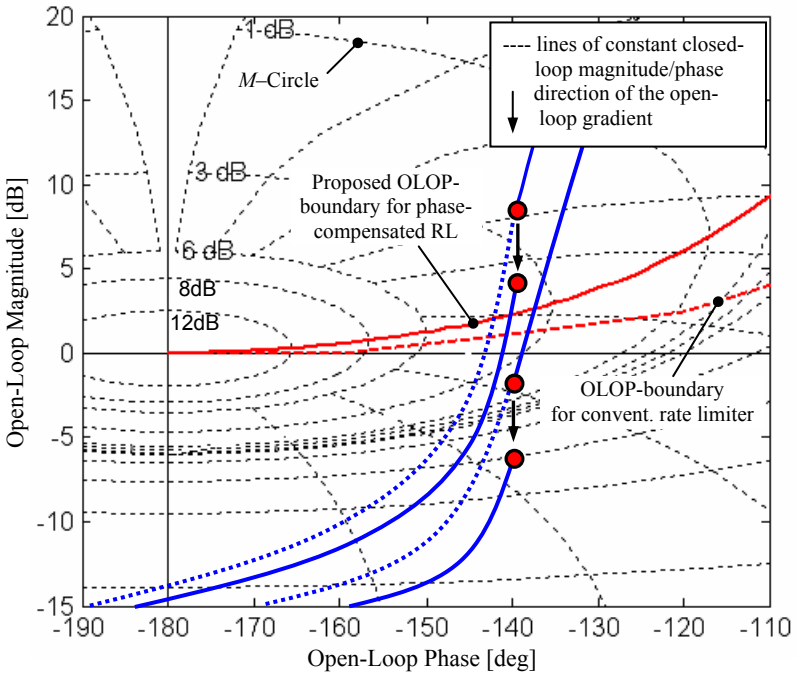

Figure 10. Nichols chart with the proposed boundary and direction of the open-loop gradient due to the activation of a phase-compensated rate limiter.

B. Validation of the Enhanced Criterion Boundary

For the validation of the proposed OLOP-boundary an OLOP-analysis (see section II) of a generic, highly augmented fighter-type aircraft is performed. To cover a wide range of different OLOP locations the open-loop frequency responses of a stable and an unstable configuration are depicted in the Nichols chart of Fig. 11 for various rate limits *R* and the same flight condition (Ma 0.6, 20 kft). Primarily, the cases above the proposed OLOP-boundary are analyzed by nonlinear simulations, as the depicted boundary is considered to be very conservative. Figure 12a shows the results of a nonlinear simulation of case #2, where the excitation function described in section II is applied. The time histories clearly show that as soon as the excitation function reaches interval II, activating the rate limiter, the aircraft response diverges. Equivalent results have been observed for cases #1 and #3. For these examples the proposed boundary is suitable to predict PIO-prone behavior. The nonlinear simulation of case #5 depicted in Fig. 12b clearly shows stable system behavior. This is also true for cases #4 and #6. Although the temporary increase of the closed-loop amplitude is clearly visible for one period as soon as the rate limiter is activated in interval II of the exciting function, the system remains stable and the amplitude is reduced again. Therefore, the increase of the closed-loop amplitude due to the open-loop gradient is not sufficient to drive the system unstable. This may require a modification of the proposed OLOP-boundary. Further case studies will be used to enhance the proposed approach.

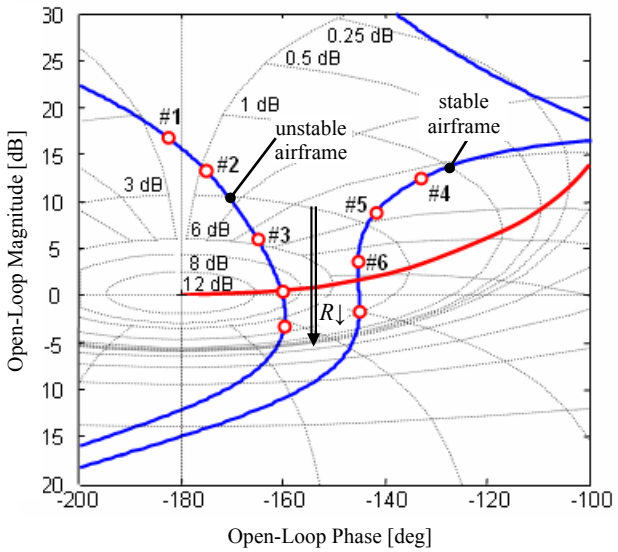

Figure 11. OLOP-analysis of two aircraft configurations with varying rate limit *R*.

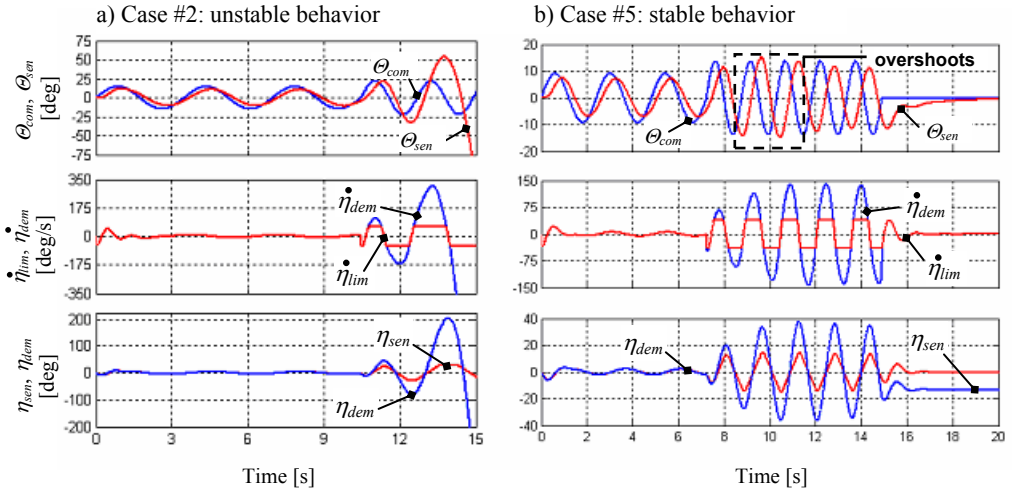

Figure 12. Nonlinear simulation results of the cases #2(a) and #5(b).

For these initial simulations additional nonlinear effects induced by position limits implemented in the feedforward and the feedback paths have not been considered to acquire a better understanding of the influences of the phase-compensated rate limiter on an otherwise linear system. Else, a clear distinction which nonlinear element has a greater impact on system stability would not be possible. In reality position limits are obviously part of every physical system (e.g. finite stick/control surface deflections). The introduction of a position limiter in the inner loop has additional deteriorating effects on overall system stability, since control power is further limited. When introducing a position limit to the feedforward path, initially unstable, PIO-critical systems may be stabilized again (for further details refer to Ref. [7]).

C. Additional Case Studies to Validate the Proposed Criterion Boundary

Two additional aircraft models are scrutinized to obtain a greater database for the definition of a new criterion boundary. Initially, a full-order X-31 model is analyzed. Subsequently, DLR's testbed ATTAS based on a VFW 614 civil transport aircraft in the configuration used for the SCARLET 3 flight test campaign conducted in 2000 is evaluated.[9]

– X-31 Aircraft

The X-31 is a highly maneuverable, statically unstable, delta canard fighter demonstrator featuring a full-authority, digital FBW FCS and a thrust vectoring nozzle, enabling post stall maneuvering. As the OLOP-criterion can only predict a possible PIO susceptibility induced by a single nonlinear element, the rate limits affecting the trailing edge flaps, being the most critical control effectors (compared to canard and thrust vectoring system) used to artificially stabilize the aircraft in pitch, are analyzed. In Fig. 13 two OLOP-frequency responses with three different rate limits are depicted. The two frequency responses have been derived for the same flight condition (cruise, Ma 0.52, 29 kft), but with different pilot gains. While for the cases #1 and #3 the actual rate limit of 60 deg/s is applied, for case #2 the rate limit has been artificially reduced to 40 deg/s.

Regarding a conventional rate limiter, an increased PIO susceptibility is predicted for cases #1 and #2, while #3 is located below the 'classical' OLOP boundary and hence should be PIO-resistant. The predictions of the OLOP-criterion for non-phase-compensated rate limiters are confirmed by nonlinear simulations for all three cases. Cases #1 and #2 show a significant destabilization of the PVS while case #3 remains stable. In Fig. 14a the time histories for case #2 are depicted, clearly showing the described instability. On the contrary, the implementation of a phase-compensated rate limiter results in stable system behavior for all three configurations, even though cases #1 and #2 are located above the proposed new boundary. Hence, the prediction of the proposed criterion boundary cannot be confirmed.

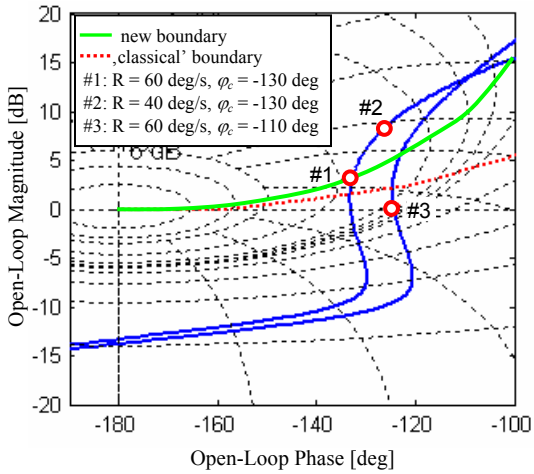

Figure 13. OLOP analyses of X-31.

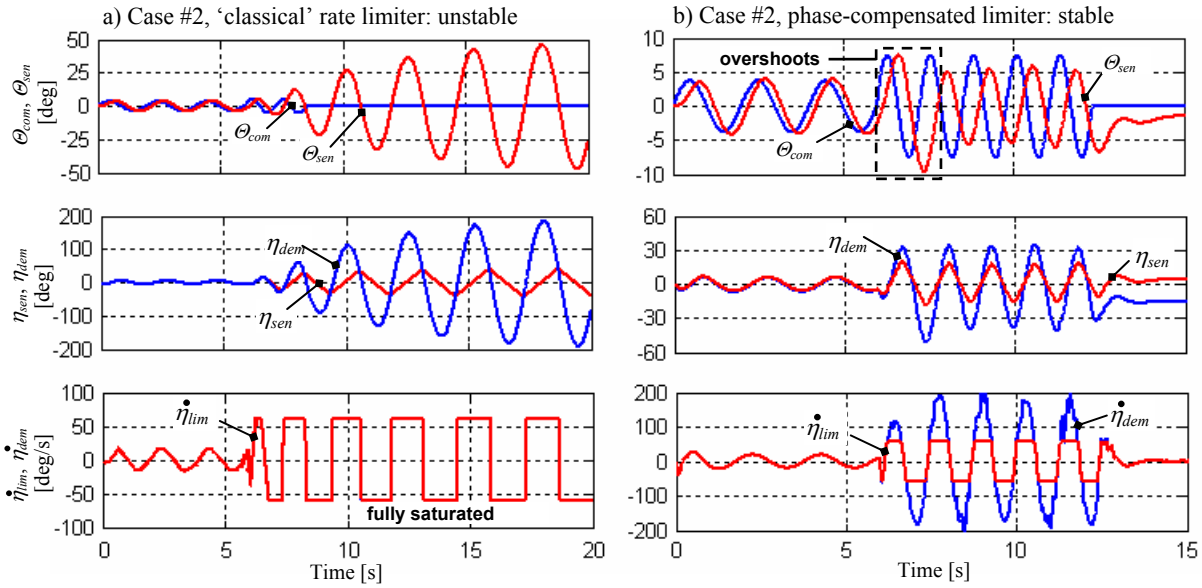

Figure 14. Nonlinear simulation results of the X-31 with conventional rate limiter (a) and a phase-compensated rate limiter (b).

The magnitude of the encountered pitch angle overshoots due to the rate limiter activation, as depicted in Fig. 14b for case #2, is different in all three cases. While for case #3 no overshoots appear at all, cases #1 and #2 show some significant pitch angle overshoots. This is evident when considering the OLOP location and the induced direction of the open-loop gradient within the Nichols chart: for cases #1 and #2 a temporary increase of the closed-loop amplitude can be observed due to the OLOP location above the proposed boundary. Case #3 is located below this line, therefore no increase of the closed-loop amplitude can be observed.

– **ATTAS Aircraft**

The ATTAS (Advanced Technologies Testing Aircraft System) is a highly modified VFW 614 operated by DLR serving as flying testbed and in-flight simulator. It features various customized systems such as direct lift control, an adaptive FBW FCS, an experimental cockpit, and extensive flight test instrumentation making it a very versatile tool to investigate new control law concepts and handling qualities. For this investigation a high fidelity aircraft model was employed resembling the aircraft configuration used during the SCARLET 3 test campaign in the year 2000.[9]

In Fig. 15 the OLOPs of the ATTAS aircraft with three different rate limits, ranging from 13 deg/s to 25 deg/s are depicted. The nonlinear simulation results with a conventional rate limiter clearly show an unstable behavior of the PVS, which confirms the predictions of the 'classical' criterion, as all OLOPs are located above the original OLOP-boundary for conventional limiters (see also Fig. 10).[9]

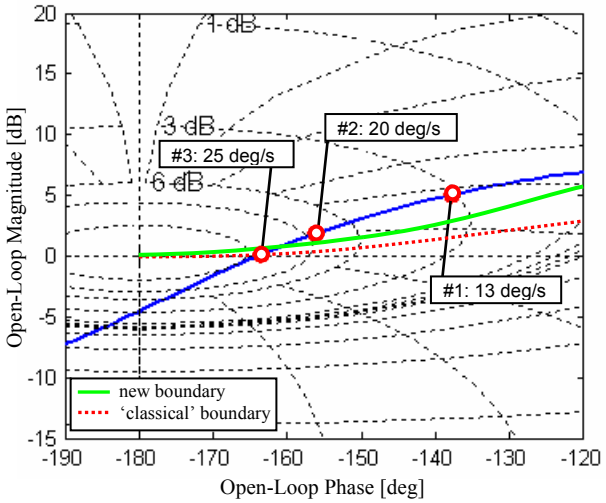

Figure 15. OLOP analyses of ATTAS with different rate limits (φ_c = -130 deg).

Considering the boundary for phase-compensated rate limiters, all three cases are located just above the newly defined criterion boundary, predicting PIO susceptibility. However, the nonlinear simulation results show stable system behavior as presented in Fig. 16 for case #2.

Due to the location of the OLOP parameter within the region where the closed-loop magnitude is rather high, in all three cases pitch angle overshoots are observed after the limiter is activated, as illustrated in Fig. 16. However, system stability is not compromised.

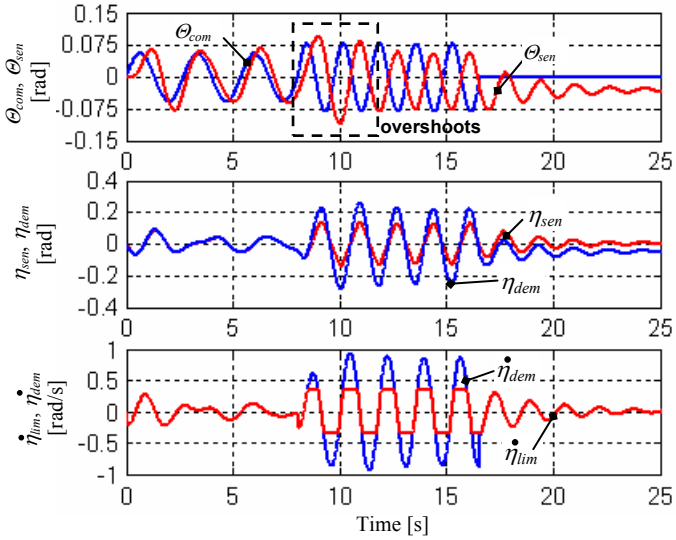

Figure 16. Nonlinear simulation of the ATTAS model (case #2) with R = 20 deg/s.

D. Definition of a new OLOP-Boundary Based on the Simulation Results

The initial validation of the proposed OLOP-boundary in the last sections has revealed the need for further adjustments. This analysis has shown that a vertical partition between PIO-free and PIO-prone configurations is required in addition to the initially proposed boundary in the Nichols chart. It is therefore suggested that the vertical portion of the boundary extends from the intersection of the initial boundary for phase-compensated rate limiters and the 6 dB *M*-circle as illustrated in Fig. 17 below. The boundary is verified by the three aircraft models described above, separating PIO-prone and PIO-free configurations. Figure 17 clearly indicates that the boundary excludes the PIO-free configurations, however, due to the limited data available for PIO-prone configurations a further displacment of the vertical boundary towards the critical point (0 dB / -180 deg) may be required. Hence, further systematic analyses have to focus on configurations with OLOPs located within the now defined PIO-prone area

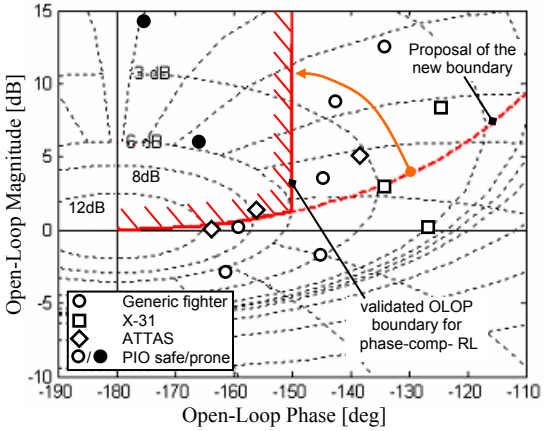

Figure 17. Proposed OLOP boundary for phase-compensated rate limiters.

V. Conclusions

Besides pointing out the advantages of phase-compensated rate limiters, which are commonly used in today's super-augmented aircraft, remaining deficiencies are identified in this paper. As these deficiencies can have tremendous influence on the system stability an adequate validation tool has been made available for the FCS design phase. Therefore, based on system-theoretical knowledge, quasi-linear and nonlinear analyses and simulations an advancement of the OLOP-criterion regarding phase-compensated rate limiters is proposed and validated using three aircraft models. For further validation, it is recommended to apply the modified/ enhanced criterion to a greater range of aircraft models which include phase-compensated rate limiters to increase the confidence level in the new criterion boundary. In particular, more PIO-prone configurations have to be validated with the modified criterion, since the boundary is assumed to be rather conservative.

Acknowledgment

The first author wants to thank his coauthors for their close support during the whole work. Also without the extensive cooperation between the German Aerospace Center (DLR) and the European Aeronautics Defence and Space Company this work would not have been possible.

References

[1] Duda, H., "Flying Qualities Criteria Considering Rate Limiting," DLR-FB 97-15, Braunschweig, 1997.

[2] Mitchell, D. G., Klyde D. H., "Recommended Practices for Exposing Pilot-Induced Oscillations or Tendencies in the Development Process," *USAF Developmental Test and Evaluation Summit*, AIAA 2004-6810, Woodland Hills, California, 2004.

[3] Gilbreath, G. P., "Prediction of Pilot-Induced Oscillations (PIO) Due to Actuator Rate Limiting Using the Open-Loop Onset Point (OLOP) Criterion," Master Thesis, Air Force Institute of Technology, Wright-Patterson Air Force Base, Ohio 2001.

[4] Slotine, J.-J. E., Li, W., Applied Nonlinear Control, Prentice Hall, Englewood Cliffs, New Jersey, 1991.

[5] Kreyszig, E., *Advanced Engineering Mathematics*, John Wiley and Sons, New York, 1993.

[6] Ossmann, D., "Investigations for the Enhancement of the Nonlinear OLOP-Criterion Regarding Phase-Compensated Rate Limiters," Project work, Technische Universität München, Institute of Flight System Dynamics, Munich, 2007 (in German).

[7] Ossmann, D., Heller, M., Brieger, O., "Handling Qualities Evaluation and PIO Prevention within the Development of Highly Augmented Aircraft," *Deutscher Luft- und Raumfahrtkongress,* DGLR-2006-112, Braunschweig 2006, pp. 281-291 (in German).

[8] Brieger, O., Kerr, M., Leißling, D., Postlethwaite, I., Sofrony, J., Turner, M., "Flight Testing of a Rate Saturation Compensation Scheme on the ATTAS Aircraft," *Deutscher Luft- und Raumfahrtkongress*, DGLR-2006-111, Braunschweig 2006, pp. 271-280.

[9] Duus, G., "SCARLET 3 - A Flight Experiment Considering Rate Saturation," *AIAA Atmospheric Flight Mechanics Conference and Exhibit*, AIAA-2000-3987, Denver, 2000, pp. 1-10.

[10] Duda, H., "Prediction of Pilot-in-the Loop Oscillations Due to Rate Saturation," *Journal of Guidance, Contro,l and Dynamics*, Vol. 20, No. 3, 1997, pp. 581-587.

[11] Committee on the Effects of Aircraft-Pilot Coupling on Flight Safety, National Research Council, *Safety And Pilot Control. Understanding and Preventing Unfavorable Pilot-Vehicle Interactions*, National Academic Press, Washington, DC, 1997, p.15.

[12] Wilmes, T., Duda. H., "Investigations of Electronic Filters to Prevent Pilot-Aircraft Coupling," DLR-IB-98/39, Braunschweig, 1998.

[13] Rundqwist, L., Hillgren, R., "Phase Compensation of Rate Limiters in JAS 39 Gripen," *AIAA Atmospheric Flight Mechanics Conference and Exhibit*, AIAA-96-3368, San Diego, 1996.

[14] Heller, M., "Lecture Notes of Control Engineering, Flight Control, Flight Mechanics and Flight Performance" FH Joanneum, Graz, 2004/2005 (unpublished/in German).